End-to-Surface Reaction Dynamics of a Single Surface-Attached DNA or Polypeptide

Ryan R. Cheng and Dmitrii E. Makarov*

Department of Chemistry and Biochemistry and Institute for Computational Engineering and Sciences, University of Texas at Austin, Austin, Texas 78712

Received: November 9, 2009; Revised Manuscript Received: February 1, 2010

The dynamics of surface-attached polymers play a key role in the operation of a number of biological sensors, yet its current understanding is rather limited. Here we use computer simulations to study the dynamics of a reaction between the free end of a polymer chain and a surface, to which its other end has been attached. We consider two limiting cases, the diffusion-controlled limit, where the reaction is accomplished whenever the free chain end diffuses to within a specified distance from the surface, and the reaction-controlled limit, where slow, intrinsic reaction kinetics rather than diffusion of the chain is rate limiting. In the diffusion-controlled limit, we find that the overall rate scales as N^{-b}, where N is the number of monomers in the chain and $b \approx 2.2$ for excluded volume chains. This value of the scaling exponent b is close to that derived from a simple approximate theory treating the dynamics of the chain end relative to the surface as one-dimensional diffusion in an effective potential. In the reaction-controlled limit, the value of the scaling exponent b is close to 1. We compare our findings with those for the related (and better studied) problem of end-to-end reactions within an unconstrained polymer chain and discuss their implications for electrochemical DNA sensors.

1. Introduction

Surface-attached biopolymers are employed in many emerging biotechnological applications, such as DNA microarrays,[1] as well as in experimental biophysical methods. For example, many optical single-molecule techniques require the molecule of interest to be immobilized on a surface.[2,3] Yet the current understanding of how surface confinement alters the dynamics and the structure of biomolecules is rather limited. In particular, theoretical work on this subject has been limited to only a handful of recent studies.[4–11] Shang and Geva, for example, have studied how tethering a freely jointed homopolymer[5] or a polypeptide[8] to either an attractive or repulsive surface affects their conformational ensemble and dynamics under varying solvent quality. Several studies of surface attachment effects on protein stability and folding kinetics have been reported.[9,10,12,13] The dynamics of a DNA tethered to a surface and subjected to a shear flow has also been studied.[11] Finally, molecular dynamics simulations of short surface-attached biopolymers have recently been reported.[6,7]

Here, we study the dynamics of a reaction occurring between one end of a polymer chain and a surface, to which the other end is attached (Figure 1a). Our interest in this problem is motivated in part by its particular application to the design of electrochemical DNA (E-DNA) sensors.[14] An E-DNA sensor is used to detect target DNA sequences and consists of an array of single-stranded DNA (ssDNA) probes. One end of each molecule is tethered to an electrode surface, while the free end is labeled with a redox group. When no complementary target DNA is present, the redox-label can collide with the electrode surface, resulting in electron transfer that can be detected by measuring the resulting Faradic current.[15] When the probes hybridize with the target DNA, the resulting double-stranded DNA (dsDNA) segment is much stiffer than the unhybridized probe, so the collisions of its end with the surface become less likely. The ensuing change in the Faradic current thus can be linked to the concentration of the target DNA.

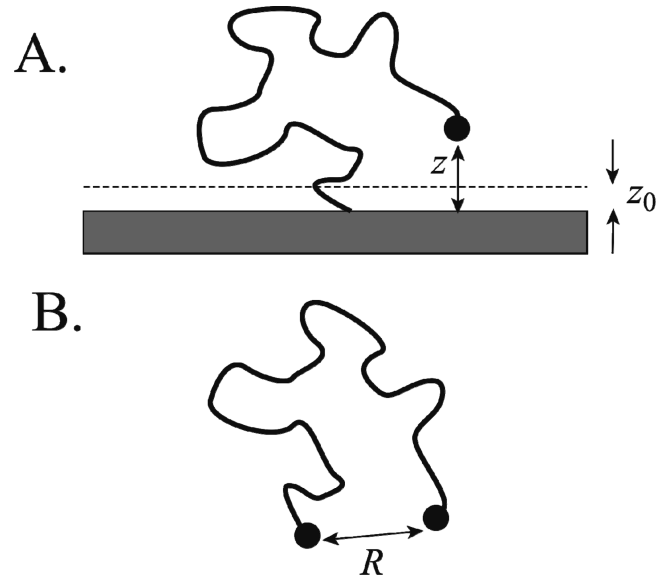

Figure 1. (a) Schematic picture of the problem studied here: One end of a polymer chain is attached to the surface. Reaction between the free chain end and the surface occurs inside a thin layer whose width is z_0. (b) A related problem of end-to-end collisions within a chain. Reaction occurs whenever the end-to-end distance is smaller than z_0.

A quantitative description of E-DNA sensors requires a theory for the dependence of the electron transfer rate on polymer properties, such as persistence length and contour length. In general, this problem is rather complex because the chain dynamics are affected by electrostatic interactions of the DNA probe with the electrode, with neighboring DNAs and with itself. Moreover, a comprehensive theory should account for the possibility of through-DNA electron transfer, in addition to the collisional mechanism described above. Our objective here is

* To whom correspondence should be addressed. E-mail: makarov@cm.utexas.edu. Fax: 512-471-8696.

10.1021/jp910669d © 2010 American Chemical Society
Published on Web 02/12/2010

more modest: We try to gain initial understanding of reaction dynamics between the chain end and the surface by considering the relatively simple case of a random-coil-like polymer attached to a hard wall-like surface.

Although, to our knowledge, this problem has not been studied in the literature (with the exception of ref 16, which considered the case of a short, stiff dsDNA that has to bend for its end to reach the surface), the related problem of end-to-end collisions within a freely diffusing polymer chain (Figure 1b) has been studied rather extensively, both experimentally[17–24] and theoretically.[25–45] In particular, the scaling of the collision rate as a function of chain length has received considerable attention and still remains a somewhat unsettled issue.[32] While brute-force computer simulations have recently provided a wealth of information about end-to-end collision dynamics,[27–29,32,46] two approximate solutions, the Wilemski−Fixman approximation[34] and the Szabo−Schulten−Schulten (SSS) theory,[47] remain useful in interpreting experimental data. The SSS theory is particularly attractive, despite its known limitations,[27,30,46] as it often allows for an analytically tractable solution. This theory assumes that the end-to-end dynamics of the polymer obeys a simple one-dimensional diffusion equation in the effective potential that correctly reproduces the distribution of the molecule's end-to-end distances.

In this paper, in addition to solving the problem of end-to surface reaction dynamics via brute-force simulations, we also seek simple approximations to describe the results. We find that SSS theory is reasonably accurate as a description of the dependence of the rate, with which the free end of the polymer chain collides with the surface, on chain length and the contact distance z_0 defined such that the collision takes place only when the distance z between the free end and the surface is less than z_0 (Figure 1a). The SSS theory, as well as dimensional analysis, further suggest that, under the assumptions that the chain is long enough and that the contact distance is greater than the bond length but shorter than the root-mean-square (rms) distance from the chain end to the surface (i.e., $\sigma \ll z_0 < \langle z^2\rangle^{1/2}$), the collision rate should be of a universal form:

$$k = t_R^{-1} f(z_0^2/\langle z^2\rangle)$$

Here t_R is the polymer's characteristic relaxation time, and $f(x)$ is a universal function, which can be fairly accurately estimated from the SSS theory. We also study the opposite limit of reaction-controlled kinetics. In this limit, slow, intrinsic reaction kinetics rather than diffusion of the chain is rate limiting. If such an intrinsic process takes place with a characteristic rate constant k_0, then we find the overall rate to obey another universal scaling relationship,

$$k = k_0 g(z_0^2/\langle z^2\rangle)$$

We note, however, that some of these findings may be model-dependent. In particular, the model adopted here accounts for excluded-volume interactions within the polymer chain but, similarly to many other common models of end-to-end collision dynamics,[19,27–29,32] neglects hydrodynamic interactions. It is known that, in the asymptotic limit of very long chains, hydrodynamic interactions can qualitatively change the physics of the end-to-end chain reactions. For example, when both excluded volume and hydrodynamic interactions are present, the diffusion-controlled limit becomes unattainable, and reaction-controlled kinetics takes place even when the intrinsic reaction kinetics is very fast.[37–39,41,42,44]

Subsequent sections of this paper will be presented as follows: Section 2 will discuss the model and methods used in our study. Sections 3 and 4 describe our results for the diffusion-controlled rate and the reaction-controlled rate, respectively. In Section 5, we compare our results with those obtained for the kinetics of reactions taking place between ends of an unconstrained polymer chain. Finally, Section 6 concludes with a discussion of the implications for DNA sensors.

2. Model and Methods

2.1. Langevin Dynamics Simulations of a Polymer Chain Attached to a Surface. Our polymer model consists of $N + 1$ beads of mass m connected by N springs, where the first bead is immobilized on the surface at $z = 0$. Here the coordinate z measures the distance from the surface as shown in Figure 1a. The pairwise interaction potential between adjacent beads separated by a distance r is taken to be harmonic:

$$V_{bond}(r) = k_{bond}(r - \sigma)^2/2 \quad (1)$$

while nonbonded beads interact via a repulsive Lennard-Jones potential representing excluded volume:

$$V_{non\text{-}bonded}(r) = 4\varepsilon[(\sigma/r)^{12} - (\sigma/r)^6]\theta(2^{1/6}\sigma - r) \quad (2)$$

Here, σ is the equilibrium bond distance, ε is a characteristic energy scale, $k_{bond} = 100.0\varepsilon/\sigma^2$, and θ is the Heaviside step function that truncates the attractive portion of the Lennard-Jones potential. The interaction between the surface and each bead (except the one that is immobilized), as a function of its distance z between the bead and the surface, is similarly represented by a repulsive Lennard-Jones potential:

$$V_{surface}(z) = 4\varepsilon[(\sigma/z)^{12} - (\sigma/z)^6]\theta(2^{1/6}\sigma - z) \quad (3)$$

The dynamics of each bead is governed by the Langevin equation

$$m\ddot{\mathbf{r}}_i(t) = -\frac{\partial V}{\partial \mathbf{r}_i} - \xi\dot{\mathbf{r}}_i(t) + \mathbf{R}_i(t) \quad (4)$$

where $\mathbf{r}_i(t)$ is the position of the bead, V is the total interaction potential, ξ is a friction coefficient, and $\mathbf{R}_i(t)$ is a random force satisfying the fluctuation−dissipation theorem. Our data is reported in reduced form where the units of length, energy, and time are σ, ε, and $\tau_0 = (m\sigma^2/\varepsilon)^{1/2}$, respectively. Simulations were performed with a temperature of $T = 1.0\varepsilon/k_B$. The value $\xi = 2.0(\sigma^2/m\varepsilon)^{-1/2}$ chosen for the friction coefficient was large enough to ensure that the dynamics were overdamped (i.e., all reaction times reported here are proportional to ξ).

2.2. The Kinetics of End-to-Surface Reaction. We assume that there is a first-order reaction between the chain end and the surface. This reaction can represent, for example, electron transfer in a DNA sensor or surface-modulated quenching of an optical probe attached to the chain end. The rate for the reaction, $k = k(z)$, depends on the distance z (Figure 1a).

Although the actual functional form of $k(z)$ depends on the specifics of the above reaction, here we will consider the

simplest possible model, where $k(z)$ is nonzero only when the distance z falls below a certain contact distance z_0, i.e.,

$$k(z) = k_0\theta(z_0 - z) \tag{5}$$

where θ is the Heaviside step function. We note that the chosen form for $k(z)$, which vanishes identically for $z > z_0$, is somewhat special, resulting in a well-defined limit $k_0 \to \infty$, where the overall measured rate becomes independent of the intrinsic rate k_0 (i.e., the diffusion controlled limit). This is not true in general.[46] Nevertheless, we adopt the simplest possible model of eq 5 to avoid the complications encountered in the more general case.[46] Simulations can of course be performed for any $k(z)$, if desired.

To describe the overall kinetics of the polymer-mediated reaction, we compute the survival probability that the reaction initiated at time t_0 has not happened by time $t_0 + t$:[48–51]

$$S(t) = \langle \exp(-\int_{t_0}^{t_0+t} k[z(t')]dt')\theta[z(t_0) - z_0]\rangle / \langle \theta(z - z_0)\rangle \tag{6}$$

The averaging, denoted by the angular brackets in eq 6, is over the canonical ensemble of initial polymer configurations at $t = t_0$, with any initial configurations that have already reacted (i.e., those with $z < z_0$) excluded by the step function in eq 6. Assuming ergodic behavior, the averages of eq 6 can also be computed from a single long polymer trajectory by performing a time average over the starting point t_0. In practice, we have performed both averages by running long trajectories on multiple processors and carrying out a time average for each. The mean first passage time for the reaction to take place is then computed as

$$\tau = \int_0^\infty S(t)dt \tag{7}$$

We are particularly interested in two limits. In the limit $k_0 \to \infty$ the result becomes independent of k_0. This is the diffusion-controlled limit, where the reaction occurs instantaneously upon the chain end, reaching the distance z_0 from the surface. The resulting diffusion-controlled rate $k_D = \tau^{-1}$ is a measure of collisions between the chain end and the surface. In practice, to compute k_D from eq 7, we use sufficiently high values of k_0 such that the mean first passage time no longer depends on k_0. Note, however, that, although the diffusion-controlled limit is well-defined for the model studied here, it is not necessarily the case in general. For example, lack of diffusion controlled limit has been predicted in loop formation within very long chains,[37–39,41,42,44] as well as the case of a more general spatial dependence of the reaction rate $k(z)$.[46]

In the opposite limit $k_0 \to 0$, the survival probability can be written as[19,48,49] $S(t) \approx \exp[-\langle k\rangle t] \equiv \exp(-k_R t)$, where

$$k_R = \langle k\rangle = \int_0^\infty k(z)p(z)dz = k_0\int_0^{z_0} p(z)dz \tag{8}$$

is the reaction controlled rate, which can be obtained by averaging $k(z)$ over the equilibrium probability distribution of the distance between the chain end and the surface. While $\tau = k_R^{-1}$ can be computed in this limit again by considering the decay of an appropriately defined survival probability, as in eqs 6−7, it is easier to calculate the reaction-controlled rate directly from eq 8. Finally, for intermediate values of k_0, one can interpolate between the diffusion- and reaction-controlled limits using the formula[19] $k = (k_D^{-1} + k_R^{-1})^{-1}$.

2.3. Estimating the Diffusion-Controlled Rate for a Gaussian Chain Using the SSS Theory.[47] In Section 3, our numerical results will be compared with the analytically solvable SSS model.[47] In this model, the free end of the chain is viewed as diffusing in a potential of mean force of the form $G(z) = -k_BT \ln p(z)$, where $p(z)$ is the equilibrium distribution of the end-to-surface distance. The first passage time to reach the contact distance z_0 and the corresponding diffusion-controlled rate constant $k_{D\text{-}SSS}$ are then given by[47]

$$\tau_{D\text{-}SSS} = k_{D\text{-}SSS}^{-1} = \int_{z_0}^\infty (D_{eff}p(z))^{-1}[\int_z^\infty p(s)ds]^2 dz \tag{9}$$

where D_{eff} is the effective diffusion coefficient along the coordinate z.

Equation 9 can be evaluated analytically for polymers obeying Gaussian statistics. Indeed, the probability distribution $p(z)$ for the distance between the free end of a Gaussian chain and a surface, to which its other end is attached, is given by[52]

$$p(z) = \left(\frac{3}{N\sigma l_K}\right)z\exp\left(-\frac{3z^2}{2N\sigma l_K}\right) \tag{10}$$

where l_K is the length of the polymer's Kuhn segment[53] (thus the mean squared end-to-end distance measured *in the absence of the surface* is equal to $N\sigma l_K$). Inserting eq 10 into eq 9, we find

$$\tau_{D\text{-}SSS} = k_{D\text{-}SSS}^{-1} = \frac{N\sigma l_K}{6D_{eff}}\Gamma\left(0, \frac{3z_0^2}{2N\sigma l_K}\right) = \frac{\langle z^2\rangle}{4D_{eff}}\Gamma\left(0, \frac{z_0^2}{\langle z^2\rangle}\right) \tag{11}$$

where Γ is the incomplete gamma function and $\langle z^2\rangle = \int_0^\infty z^2 p(z)dz = (2/3)N\sigma l_K$ is the mean square distance between the chain end and the surface.

In order to use eq 11 to predict the diffusion-controlled collision rate in our model, we need two parameters, the Kuhn length l_K and the effective diffusion coefficient D_{eff}. The former can be estimated by fitting the mean squared end-to-end distance of the chain (in the absence of the surface) with $N\sigma l_K$. The latter can be estimated by comparing the behavior of the autocorrelation function of the end-to-surface distance $z(t)$ for polymer model with that expected for the one-dimensional diffusion model.[54] Specifically, using a harmonic approximation for the potential of mean force

$$G(z) = -k_BT \ln p(z) = G(z_m) + (1/2)G''(z_m)(z - z_m)^2 \tag{12}$$

where $z_m = (N\sigma l_K/3)^{1/2}$ corresponds to the maximum of $p(z)$, one can estimate the effective diffusion coefficient as[54]

$$D_{eff} = \frac{k_BT}{G''(z_m)}\frac{C(0)}{\int_0^\infty C(t)dt} \tag{13}$$

where

$$C(t) = \langle z(t)z(0)\rangle - \langle z\rangle^2 \tag{14}$$

The correlation function of eq 14 can be often approximated by a single exponential,

$$C(t) = C(0)\exp(-t/t_0) \tag{15}$$

We have directly tested eq 15 by simulations and found that it always holds well. If we further assume that our Gaussian polymer obeys Rouse dynamics (i.e., Brownian dynamics, with hydrodynamic effects neglected[55]), then we expect that $C(t)$ would be dominated by the slowest Rouse relaxation mode so that $t_0 = t_R$, where

$$t_R = \frac{N^2\sigma l_K \xi}{3\pi^2 k_B T} \tag{16}$$

is the Rouse relaxation time of the chain. Indeed, neglecting faster relaxation modes in the expression for $C(t)$ results in a fairly small error (~10%) when estimating the effective end-to-end diffusion coefficient of a free Rouse chain.[54] However, this result has to be modified to account for the fact that one end of the chain is fixed. This leads to a different boundary condition for the Rouse relaxation modes.[56] Consequently, for a Rouse chain with one end fixed, the corresponding slowest relaxation time is not t_R but $t_0 = 4t_R$.[56] Using eqs 13−16, one finds

$$D_{eff} \approx \frac{k_B T}{G''(z_m)t_0} = \frac{N\sigma l_K}{6t_0} = \frac{N\sigma l_K}{24 t_R} = \frac{\pi^2}{8}\frac{k_B T}{N\xi} \tag{17}$$

Similarly to the free Rouse chain, D_{eff} of a constrained chain is inversely proportional to chain length.[54]

3. Results: The Diffusion-Controlled Rate k_D

3.1. Dependence of the Diffusion-Controlled Rate on Chain Length N and the Contact Distance z_0. In the diffusion-controlled limit, the reaction kinetics are determined by the collisions of the free chain end with the surface, where a collision is defined as an event in which the chain end approaches the surface to within the contact distance z_0. The mean first passage time τ to such a collision is related to the usual diffusion-controlled rate,[47] $k_D = \tau^{-1}$. For sufficiently small values of z_0 and/or long chains, the chain length dependence of k_D is well approximated by a power law

$$k_D \propto N^{-b} \tag{18}$$

where the value of the exponent b is close to 2.16 (Figure 2, the case $z_0 = 2^{7/6}\sigma$). Deviations from a power law dependence become significant as z_0 is increased and becomes comparable with the typical distance z between the surface and the chain end.

The SSS rate $k_{D\text{-}SSS}$ (eqs 11 and 17), while being off roughly by an order of magnitude for the longest chains studied, reproduces remarkably well both the scaling exponent b in the limit of small z_0 and the deviations from the power law observed at larger values of z_0 and/or for short chains.

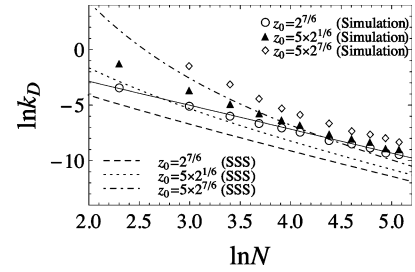

Figure 2. In the limit where the chain length is long enough that the typical distance z from its end to the surface is much longer than the contact distance z_0, the diffusion-controlled rate k_D scales as $k_D \propto N^{-b}$ (solid line) where b is close to 2.16. Deviations from this power law are observed when the typical values of z become comparable to z_0. The SSS theory (dashed lines) describes well both the asymptotic power law and departures from this law observed at large z_0 and small N.

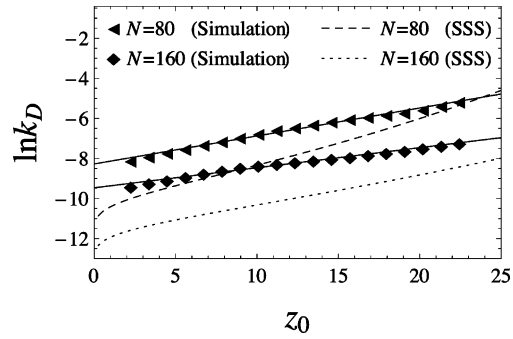

Figure 3. The diffusion controlled rate k_D increases (approximately exponentially) with the contact distance z_0. SSS predicts similar behavior, although the functional dependence on z_0 is not exponential (eq 11).

Likewise, the dependence of the diffusion-controlled rate on the contact distance z_0 is well captured by the SSS theory (Figure 3). Although this dependence appears to be well approximated by an exponential function $k_D \propto e^{az}$ (solid lines in Figure 3), this behavior may be accidental. Indeed, the SSS prediction of eq 11 also appears to behave exponentially in the same range of z_0, while the actual analytical formula is inversely proportional to an incomplete Gamma function involving z_0^2 and is not an exponential function of z_0.

When extrapolated to $z_0 \to 0$, our numerical data for k_D appears to predict a finite value of the diffusion-controlled rate. This simple extrapolation is obviously incorrect, as the probability of finding the end monomer at $z = 0$ is identically equal to zero, and so collisions defined by $z_0 = 0$ never happen. In contrast, the SSS rate of eq 11 exhibits physically reasonable behavior and vanishes at $z_0 \to 0$. The regime of small contact distances that are shorter than or comparable to the monomer size is physically quite different from the regime considered here. For $z_0 < \sigma$, the properties of the distribution $p(z)$ are strongly dependent on the interaction potential between the end monomer and the surface. Therefore, the behavior of k_D can be strongly model-dependent. In contrast, results should become less model dependent when the contact distance z_0 exceeds a typical length scale of surface−monomer interactions. Below we propose that, for $z_0 \gg \sigma$ and $N \gg 1$, the dependence $k_D(N,z_0)$ can indeed be written in a simple, universal form.

3.2. Dimensional Analysis of $k_D(N,z_0)$. Let us first ignore excluded volume interactions among the nonbonded beads of the chain. Assuming an overdamped limit (i.e., neglecting the first term in eq 4) and taking the long chain limit ($N \gg 1$), our

model becomes equivalent to the standard Rouse model.[55] Treating the monomer number n as continuous, relaxation of the chain is then described by the equation[53,55]

$$\frac{\partial \mathbf{r}_n}{\partial t} = \frac{\pi^2 N^2}{t_R}\frac{\partial^2 \mathbf{r}_n}{\partial n^2} \tag{19a}$$

where $\mathbf{r}_n$ is the position of the nth monomer and t_R is the Rouse time defined in eq 16. For a chain with one end fixed, the boundary conditions are: $\mathbf{r}_0 = 0$ (monomer does not move) and $(\partial \mathbf{r})/(\partial n)|_{n=N} = 0$ (zero force on the free end). This leads to the solutions of the form $\mathbf{r}_n(t) \sim \exp(-t/t_p)\sin[\pi(1/2 + p)n/N]$, $p = 0,1...$, where the relaxation times are given by $t_p = t_R/(1/2 + p)^2$. The lowest relaxation time is thus $t_0 = 4t_R$, as already pointed out in Section 2.3.

In the reduced units $\zeta = n/N$, $T = t/t_R$, and $\rho(\zeta) = \mathbf{r}_n/\langle z^2\rangle$, eq 19a becomes invariant with respect to chain length:

$$\frac{\partial \rho}{\partial T} = \frac{1}{\pi^2}\frac{\partial^2 \rho}{\partial \zeta^2} \tag{19b}$$

Likewise, when viewed at a spatial resolution that is coarser than the monomer length scale σ, the spatial properties of the chain (in particular the spatial distribution of z) are invariant when the distances are normalized by the only remaining characteristic length scale $\langle z^2\rangle^{1/2}$ (see, e.g., refs 53 and 57)). We thus expect that, for $z_0 \gg \sigma$, the first passage time τ, when scaled by t_R, should be a dimensionless quantity that only depends on the dimensionless ratio $u = z_0/\langle z^2\rangle^{1/2}$, i.e.,

$$\tau/t_0 = \tau/(4t_R) = 1/f(u) \quad \text{or} \quad k_D t_0 = f(u) \tag{20}$$

where $f(u)$ is some yet unknown function.

The SSS approximation for the diffusion-controlled rate is precisely of the form of eq 20. Indeed, using eq 17, eq 11 can be rewritten in the form of eq 20, where

$$f(u) = 1/\Gamma(0, u^2) \tag{21}$$

We now surmise that eq 20 should be valid even in the more general case where the polymer is not Gaussian, provided that a characteristic polymer reconfiguration time scale t_0 is appropriately defined. Specifically, we can estimate t_0 by fitting the autocorrelation function of eq 14 by an exponential (cf. eq 15).

If our hypothesis is correct, all of the data shown in Figure 2 should collapse onto a single curve when plotted as $k_D t_0$ versus $u = z_0/\langle z^2\rangle^{1/2}$. Replotting Figure 2 this way, we do not find a perfect collapse (Figure 4). Nevertheless, deviations from a hypothetical single curve observed in Figure 4 are less than a factor of 2, while the rate k_D itself spans many orders of magnitude (cf. Figure 2). It is likely that the lack of perfect collapse can be attributed to the fact that the asymptotic $N \to \infty$ behavior has not been attained for our chains; indeed, it has been previously observed[54] that finite-size effects may persist in the statistics of spatially confined polymer chains even when the latter are hundreds of times longer than the Kuhn segment. An ultimate resolution of this issue would be to perform simulations with much longer chains but, unfortunately, it is impractical to obtain statistically accurate data for such long chains given our central processing unit (CPU) resources. Given

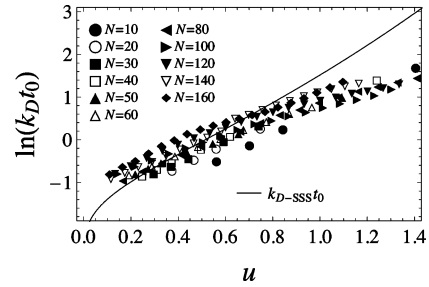

Figure 4. For sufficiently long chains, we expect the rescaled rate $k_D t_0$ to asymptotically approach a universal relation when plotted as a function of the dimensionless parameter $u = z_0/\langle z^2\rangle^{1/2}$. Here we test this prediction and find that this collapse is not perfect for the chains of the lengths as long as $N = 160$ monomers studied here, presumably because of finite-size effects. The solid line represents a plot of $k_{D\text{-SSS}}t_0 = 1/\Gamma(0,u^2)$ predicted by the SSS theory (eq 11).

these limitations, nevertheless, it is important to point out that, for sufficiently short contact distances relative to the typical size of the polymer chain (i.e., for $u \leq 1$), the SSS-derived universal curve predicted by eq 21 describes all of our data to within a factor of 2.

These findings allow us now to better understand the origins of the power law for the rate k_D as a function of chain length N. Consider the limit where the contact distance z_0 is much shorter than the characteristic polymer size $\langle z^2\rangle^{1/2}$ (i.e., when $u \ll 1$) but still longer than the monomer size σ. The function $f(u)$ is only weakly dependent on u in this limit. For example, the SSS prediction for $f(u)$ (eq 21) gives logarithmic dependence in this regime:

$$f(u) \approx -(2\ln u + \gamma)^{-1} \tag{22}$$

where $\gamma \simeq 0.577$ is Euler's constant. If we neglect this weak dependence, then, according to eq 20, the diffusion-controlled rate should scale as $1/t_R$. For a Rouse chain with excluded volume, the scaling of t_R has been predicted[57] to be of the form $t_R \propto \langle R^2\rangle/D \propto N^{1+2\nu} \approx N^{2.2}$, where $\nu \approx 3/5$ is Flory's scaling exponent,[53] R is the polymer's end-to-end distance, and D is the diffusion coefficient for the entire chain. Thus we expect the scaling of the form $k_D \propto N^{-2.2}$ for excluded-volume polymer chains. The actual scaling exponent estimated numerically (Figure 2) is indeed close to this prediction. When u is no longer small, then the chain length dependence of $f(u)$ can no longer be neglected. This leads to a stronger chain length dependence of the overall rate constant k_D and to deviations from the simple power law of eq 18 (Figure 2).

We finally note that similar $1/t_R$ scaling has been predicted for the related problem of the diffusion-controlled rate of end-to-end collisions in a freely diffusing chain.[26,28,32,39] We will further compare these two cases in Section 5.

4. Results: The Reaction-Controlled Rate k_R

Similarly to the diffusion controlled rate, the reaction-controlled rate k_R (eq 8) exhibits a power law behavior, $k_R \propto N^{-c}$, with the exponent c close to 1, provided that z_0 is much smaller than the typical end-to-surface distances z (Figure 5). This scaling exponent is also close to that estimated for a Gaussian chain. This can be seen by substituting the distribution $p(z)$ from eq 10 into eq 8, which gives

$$\frac{k_R}{k_0} = 1 - \exp(-u^2), \quad u = \frac{z_0}{\langle z^2 \rangle^{1/2}} \tag{23}$$

For $z_0 \ll \langle z^2 \rangle^{1/2}$, this equation predicts $k_R/k_0 \approx u^2 = z_0^2/\langle z^2 \rangle \propto 1/N$ since $\langle z^2 \rangle \propto N$ for a Gaussian chain. Crudely speaking, k_R is proportional to the probability $p(z_0)$ of finding the chain's end within the required distance from the surface, which, according to eq 10, is proportional to $1/N$ for Gaussian chains. Curiously, our data indicates that the $\approx 1/N$ scaling is rather robust and insensitive to the chain statistics (Figure 5). Moreover, the same scaling is found in the opposite extreme in which the chain is very stiff and behaves like a rigid rod of length L. Indeed, for a rigid rod that is free to pivot around its attachment to the surface, the probability distribution $p(z)$ is given by $p(z) = (2/\pi L)(1 - z^2/L^2)^{1/2} \approx 2/(\pi L)$. Thus the rate k_R scales again as $1/L \propto 1/N$.

Regardless of whether excluded volume effects are present, the reaction controlled rate for sufficiently long chains satisfies the scaling relationship

$$k_R/k_0 = g(u) = g(z_0/\langle z^2 \rangle^{1/2}) \tag{24}$$

provided that z_0 is greater than the monomer size. This scaling relationship immediately follows from eq 8 and from the fact that $p(z)$ is of the general form[53,57] $p(z) = \langle z^2 \rangle^{-1/2} h(z/\langle z^2 \rangle^{1/2})$, where $h(x)$ is another dimensionless function.

Consistent with the above prediction, the data of Figure 5, when replotted as k_R/k_0 versus u, collapses onto a universal curve $g(u)$ (Figure 6). Moreover, the relationship $g(u) = 1 - \exp(-u^2)$ predicted for ideal chains (eq 23) describes the data reasonably well even in the presence of excluded volume effects.

5. End-to-Surface versus End-to-End Reaction

Although collisions of the free end of a surface-attached DNA with the respective surface are believed to provide the mechanism through which target-induced structural changes are detected in E-DNA sensors (see, e.g., refs 14 and 15), very little experimental information is currently available about the basic physics of this process. In contrast, collisions between the ends of an unconstrained biopolymer (ssDNA or protein) in solution have received considerable experimental attention.[17–19,22,24,58] It is therefore natural to ask whether the current understanding of end-to-end reaction dynamics (Figure 1b) is transferrable to the problem of an end-to-surface reaction (Figure 1a). To answer this question, here we compare the simulation results reported in the previous sections with end-to-end reaction rates for the same polymer chains. For the latter process, we have adopted

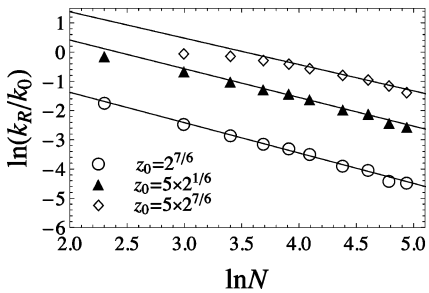

Figure 5. Chain length dependence of the reaction-controlled rate k_R is close to inversely proportional. The solid lines are power law fits N^{-b}, where $b = 1.04$, 0.981, and 0.901 for $z_0 = 2^{7/6}\sigma$, $z_0 = 5 \times 2^{1/6}\sigma$, and $z_0 = 5 \times 2^{7/6}\sigma$, respectively.

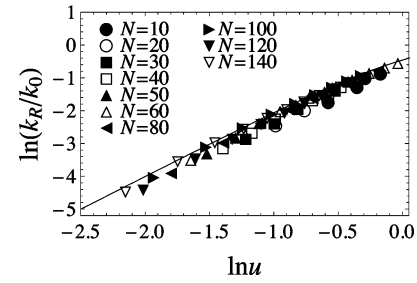

Figure 6. k_R/k_0 approaches a universal relation when plotted as a function of the dimensionless parameter $u = z_0/\langle z^2 \rangle^{1/2}$. The solid line is the analytical prediction for Gaussian chains eq 23

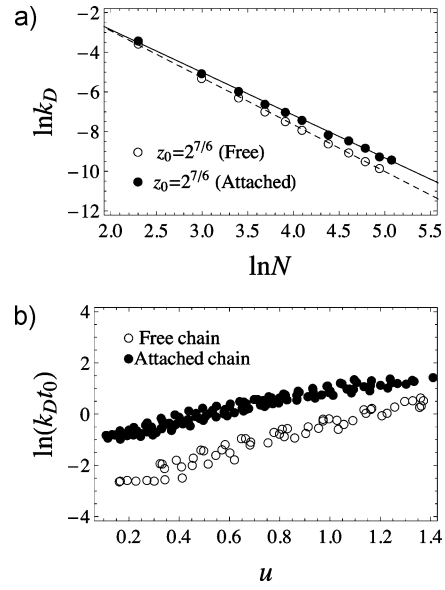

Figure 7. (a) End-to-end collisions of a free chain and end-to-surface collisions of a tethered chain show similar chain length dependence in the diffusion controlled regime. Here, $k_D \propto N^{-2.37}$ and $N^{-2.16}$ in the former and latter cases for $z_0 = 2^{7/6}\sigma$. (b). The diffusion-controlled rate of end-to-end collisions for a free chain and end-to-surface collisions of a tethered chain exhibit similar (near) universal dependence on the reduced parameter $u = z_0/\langle z^2 \rangle^{1/2}$ when measured in reduced time units set by the polymer relaxation time scale t_0. The data for surface attached chains are the same as in Figure 4.

a model analogous to that described in Section 2.2. Specifically, we have assumed that a chain-mediated end-to-end reaction has an end-to-end distance-dependent rate described by eq 5, where z is replaced by the distance R between the end monomers of the polymer (Figure 1b). The parameter z_0 is now interpreted as a "capture radius" such that no reaction occurs if the end-to-end distance exceeds it. The results for end-to-end rates reported here were obtained through a straightforward modification of the procedures described in Section 2: eqs 6−8 were used to compute the diffusion- and reaction-controlled rates by simply removing the surface constraint and replacing z by R.

The scaling of the diffusion controlled rate with chain length N is very similar in the cases of end-to-end collisions in unconstrained polymers and of end-to-surface collisions of surface-attached polymers (Figure 7a). This result is not surprising: According to earlier theoretical predictions for unconstrained polymers[26,32,39] and to the scaling considerations of Section 3, k_D should roughly scale as $1/t_R$ in each case, resulting in a similar chain length dependence (eq 18) with a scaling exponent close to $b = 2.2$. For sufficiently small z_0, we find that the end-to-surface rate is always greater than the end-to-end rate. Again, this result is not surprising since a surface

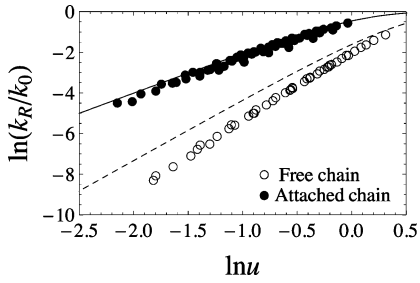

Figure 8. In the reaction controlled regime, the rate of an end-to-end reaction for an unconstrained chain has a stronger chain length dependence than that of an end-to-surface reaction of a surface tethered chain, according to both numerical simulations (circles) and analytical theory for Gaussian chains (lines). Here, these rates are plotted as a function of the dimensionless parameter $u = z_0/\langle z^2\rangle^{1/2}$, which itself scales as $u \propto N^{-\nu}$(where $\nu = 1/2$ and 3/5 for Gaussian and excluded-volume chains, respectively).

presents a larger target for a chain end to strike, as compared to the other end monomer of the chain.

Just as in the case of collisions with a surface, the end-to-end diffusion controlled rates measured for chains of varying length and capture radius z_0 fall close to a universal curve when properly rescaled. Specifically, we find a relationship of the form (Figure 7b)

$$k_D t_0 \approx \tilde{f}(u) \tag{25}$$

Similarly to the case of surface-attached chains, the parameter u for an unconstrained chain is defined as the ratio of z_0 to the rms chain extension in the z direction (which is now equivalent to the x- and y-directions)

$$u^2 = z_0^2/\langle z^2\rangle = 3z_0^2/\langle R^2\rangle \tag{26}$$

The relaxation time t_0 was determined by fitting the autocorrelation function of the end-to-end distance to an exponential, similarly to eqs 14−15. The function $\tilde{f}(u)$ defined this way behaves very similarly to the function $f(u)$ found for end-to-surface collisions (Figure 7b). For the same values of t_0 and u, the rate of end-to-surface collisions is roughly an order of magnitude higher than that of end-to-end collisions (Figure 7b).

Similarly to the case of diffusion-controlled rates, the reaction-controlled rate k_R for an end-to-end reaction is smaller than that for an end-to-surface reaction (Figure 8). In contrast to the diffusion-controlled rate, however, the scaling of the reaction-controlled rate as a function of chain length is quite different for end-to-end and end-to-surface reactions. This difference in scaling is readily understood by considering the case of a Gaussian chain. For a surface-attached Gaussian chain, the rate k_R is given by eq 23. For long chains this rate thus scales as $k_R \propto u^2 \propto N^{-1}$. In contrast, the reaction controlled end-to-end rate for a Gaussian chain is given by (cf. eq 8)

$$k_R/k_0 = \int_0^{z_0} p(r)dr = \int_0^{z_0} 4\pi r^2 \left(\frac{2\pi\langle R^2\rangle}{3}\right)^{-3/2} \times \exp\left(\frac{-3r^2}{2\langle R^2\rangle}\right)dr = \mathrm{erf}\left[\frac{u}{\sqrt{2}}\right] - \left(\frac{2}{\pi}\right)^{1/2} u \exp\left(-\frac{u^2}{2}\right) \tag{27}$$

For $u \ll 1$, this results in chain length dependence given by $k_R \propto u^3 \propto N^{-3/2}$. These scaling laws are easy to understand: As noted in Section 4, the reaction-controlled rate is proportional to the probability of finding the reacting entities in close proximity. This probability scales as $1/N$ for a chain end reacting with the surface and as $N^{-3/2}$ for one chain end reacting with the other. Consequently, an end-to-end reaction exhibits a significantly stronger dependence on chain length as compared to its end-to-surface analog in the reaction limited regime. This conclusion remains true when excluded volume effects are taken into account (see Figure 8). Interestingly, the Gaussian chain approximation works reasonably well in the case of a surface-attached chain (eq 23), while it is considerably less accurate in the case of an end-to-end reaction within an unconstrained polymer.

6. Concluding remarks

Our study was largely motivated by the recently developed E-DNA method of detecting ssDNA.[14,15] In this technique, an ssDNA probe attached to an electrode surface undergoes hybridization with a free DNA thus resulting in the formation of a dsDNA tethered to the surface. This changes the electron transfer rate between the redox-modified free DNA end and the surface, which is manifested as a change in the Faradic current. To understand this change more quantitatively, first note that the Kuhn length l_K of dsDNA is much longer than that of ssDNA.[59] Since, depending on the intrinsic rate of electron transfer, both reaction-limited and diffusion-limited regimes are possible, below we consider both cases separately.

Diffusion-Controlled Case. Using eqs 20−21 and omitting numerical factors, we can write the diffusion-limited rate as

$$k_D \propto t_0^{-1} f(z_0/\langle z^2\rangle^{1/2}) = t_0^{-1} f(u) \tag{28}$$

The characteristic chain relaxation time can often be approximated by the following scaling relationship[53] (eq 16 being its particular case for the Rouse model):

$$t_0 \propto \langle R^2\rangle/D_{\mathrm{chain}} \tag{29}$$

where $\langle R^2\rangle$ is the mean square end-to-end distance and D_{chain} is the diffusion constant of the entire chain. Using $\langle R^2\rangle \sim \sigma l_K N$ we find that the factor t_0^{-1}in eq 28 is roughly inversely proportional to the Kuhn length and thus should decrease upon DNA hybridization. In addition, it is plausible that the diffusion coefficient D_{chain} for a dsDNA is lower than that of an ssDNA of the same length, thus providing further hybridization-induced reduction of k_D. Finally, since $f(u)$ is a monotonically increasing function of the parameter

$$u = z_0/\langle z^2\rangle^{1/2} \propto z_0/(N\sigma l_K)^{1/2} \tag{30}$$

the last factor in eq 28 will also decrease upon DNA hybridization. All these effects will result in a reduction of the Faradic current, consistent with the experimental observations.[14,15]

Reaction-Limited Case. In this limit, we can use eq 23 to estimate the dependence of the rate k_R on the polymer Kuhn length. If we further assume that $z_0 \ll \langle z^2\rangle^{1/2}$, then we find

$$k_R \propto \langle z^2\rangle^{-1} \propto l_K^{-1} \tag{31}$$

Like in the diffusion-controlled case, the reaction-controlled rate decreases with increasing Kuhn length, but this dependence is somewhat weaker than for the diffusion-limited rate.

The Limit of Stiff dsDNA. In the above estimates, we assumed that the polymer contour length $L = N\sigma$ is much longer than its Kuhn length so that both the ssDNA and the dsDNA are flexible. However, while the Kuhn length of ssDNA typically corresponds to just a few bases, the Kuhn length of dsDNA corresponds to over 100 base pairs, which is longer than the length of the DNA constructs commonly employed in DNA sensors. For such short and therefore stiff DNA, the end-to-surface collision rate strongly depends on the manner in which the molecule is attached to the surface. For example, if the molecule is not free to pivot around the attachment point, then a collision of its end with the surface will involve surmounting an energy barrier required to bend the molecule. This scenario has been studied in ref 16. Here we consider the opposite case of a dsDNA approximated as a rigid rod freely pivoting around its surface attachment. The diffusion limited rate can be crudely estimated using a relationship similar to eq 29, as the inverse time it takes the whole chain to diffuse over the distance comparable to its own size:

$$k_{\mathrm{D,dsDNA}} \sim \frac{D_{\mathrm{chain,dsDNA}}}{L^2} \tag{32}$$

where $L = N\sigma$ is the length of the molecule. To compare this result with the end-to-surface collision rate for ssDNA of the same contour length, we can use eqs 28−29. If we further neglect the weak dependence of $f(u)$ and replace it by a constant, we can write

$$k_{\mathrm{D,ssDNA}} \sim \frac{D_{\mathrm{chain,ssDNA}}}{\langle R^2 \rangle} = \frac{D_{\mathrm{chain,ssDNA}}}{N\sigma l_{\mathrm{K,ssDNA}}} \tag{33}$$

Comparing eqs 32 and 33, we find that $k_{\mathrm{D,ssDNA}} \gg k_{\mathrm{D,dsDNA}}$ as long as the contour length of the DNA is longer than the Kuhn length of ssDNA, $L = N\sigma \gg l_{\mathrm{K,ssDNA}}$.

In the reaction-controlled limit, we use the fact that the probability that the free end of a rigid rod is within a distance $z_0 \ll L$ from the surface is given by $\sim p(0)z_0 \approx 2z_0/(\pi L)$ (see Section 4). Thus the reaction-limited rate is given by $k_{\mathrm{R,dsDNA}} \propto k_0 z_0/L$, which, again, should be compared with the ssDNA rate estimated from eq 23, $k_{\mathrm{R,ssDNA}} = k_0 z_0^2/(N\sigma l_{\mathrm{K,ssDNA}})$. Comparing the two rates, we find that $k_{\mathrm{R,ssDNA}} \gg k_{\mathrm{R,dsDNA}}$ as long as $z_0 \gg l_{\mathrm{K,ssDNA}}$. The latter inequality, however, is not necessarily satisfied under experimental conditions. Indeed, if the process in question involves electron transfer, the corresponding characteristic length scale may be very short, on the order of a few angstroms shorter than the typical Kuhn length of ssDNA. The case $z_0 < l_{\mathrm{K,ssDNA}}$ would have to be dealt with much more carefully. In particular, eq 23 is likely to be inadequate in this case because the probability distribution $p(z)$ for such short distances would be affected by the specifics of the polymer−surface interaction. Finally, since the dynamics of dsDNA is effectively slower than that of ssDNA, it is also conceivable that a transition from reaction-controlled to diffusion-controlled electron transfer kinetics can happen upon DNA hybridization. Further understanding of how DNA hybridization affects the electron transfer rate in E-DNA sensors will require more realistic polymer models as well as knowledge of the specifics of the electron transfer system employed (such as the intrinsic quenching rate and its distance dependence).

Acknowledgment. R.R.C. was supported by the Robert A. Welch Foundation (through Grant F-1514 to D.E.M.). D.E.M. was supported by the NSF Grant CHE 0848571. We are indebted to Kevin W. Plaxco and Takanori Uzawa for drawing our attention to this problem and for many discussions. The CPU time was provided by the Texas Advanced Computer Center.

References and Notes

(1) Heller, M. J. *Annu. Rev. Biomed. Eng.* **2002**, *4*, 129.
(2) Rasnik, I.; McKinney, S. A.; Ha, T. *Acc. Chem. Res.* **2005**, 38.
(3) Talaga, D. S.; Lau, W. L.; Roder, H.; Tang, J.; Jia, Y.; DeGrado, W. F.; Hochstrasser, R. M. *Proc. Natl. Acad. Sci. U.S.A.* **2000**, *97*, 13021.
(4) Eisenriegler, E.; Kremer, K.; Binder, K. *J. Chem. Phys.* **1982**, *77*, 6296.
(5) Shang, J.; Geva, E. *J. Phys. Chem. B* **2005**, *109*, 16340.
(6) Feng, J.; Wong, K. Y.; Lynch, G. C.; Gao, X.; Pettitt, B. M. *J. Phys. Chem. B* **2007**, *111*, 13797.
(7) Wong, K. Y.; Pettitt, B. M. *Biopolymers* **2004**, *73*, 570.
(8) Shang, J.; Geva, E. *J. Phys. Chem. B* **2007**, *111*, 4178.
(9) Friedel, M.; Baumketner, A.; Shea, J.-E. *Proc. Natl. Acad. Sci. U.S.A.* **2006**, *103*, 8396.
(10) Zhuang, Z.; Jewett, A. I.; Soto, P.; Shea, J.-E. *Phys. Biol.* **2009**, 6.
(11) Zhang, Y.; Donev, A.; Weisgraber, T.; Alder, B. J.; Graham, M. D.; De Pablo, J. J. *J. Chem. Phys.* **2009**, 130.
(12) Knotts IV, T. A.; Rathore, N.; De Pablo, J. J. *Proteins: Structure, Function, and Bioinformatics* **2005**, *61*, 385.
(13) Knotts IV, T. A.; Rathore, N.; de Pablo, J. J. *Biophys. J.* **2008**, *94*, 4473.
(14) Fan, C.; Plaxco, K. W.; Heeger, A. J. *Proc. Natl. Acad. Sci. U.S.A.* **2003**, *100*, 9134.
(15) Ricci, F.; Lai, R. Y.; Plaxco, K. W. *Chem. Commun.* **2007**, 3768.
(16) Anne, A.; Demaille, C. *J. Am. Chem. Soc.* **2005**, *128*, 542.
(17) Bieri, O.; Wirz, J.; Hellrung, B.; Schutkowski, M.; Drewello, M.; Kiefhaber, T. *Proc. Natl. Acad. Sci. U.S.A.* **1999**, *96*, 9597.
(18) Lapidus, L. J.; Eaton, W. A.; Hofrichter, J. *Proc. Natl. Acad. Sci. U.S.A.* **2000**, *97*, 7220.
(19) Lapidus, L. J.; Steinbach, P. J.; Eaton, W. A.; Szabo, A.; Hofrichter, J. *J. Phys. Chem. B* **2002**, *106*, 11628.
(20) Wang, X. J.; Nau, W. M. *J. Am. Chem. Soc.* **2004**, *127*, 13232.
(21) Kawai, K.; Yoshida, H.; Sugimoto, A.; Fujitsuka, M.; Majima, T. *J. Am. Chem. Soc.* **2005**, *127*, 13232.
(22) Uzawa, T.; Cheng, R. R.; Cash, K. J.; Makarov, D. E.; Plaxco, K. W. *Biophys. J.* **2009**, *97*, 205.
(23) Soranno, A.; Longhi, R.; Bellini, T.; Buscaglia, M. *Biophys. J.* **2009**, *96*, 1515.
(24) Fierz, B.; Kiefhaber, T. *J. Am. Chem. Soc.* **2007**, *129*, 672.
(25) Chen, J. Z. Y.; Tsao, H.-K.; Sheng, Y.-J. *Phys. Rev. E* **2005**, *72*, 031804.
(26) Doi, M. *Chem. Phys.* **1975**, *9*, 455.
(27) Pastor, R. W.; Zwanzig, R.; Szabo, A. *J. Chem. Phys.* **1996**, *105*, 3878.
(28) Podtelezhnikov, A.; Vologodskii, A. *Macromolecules* **1997**, *30*, 6668.
(29) Portman, J. J. *J. Chem. Phys.* **2003**, *118*, 2381.
(30) Sokolov, I. M. *Phys. Rev. Lett.* **2003**, *90*, 080601.
(31) Thirumalai, D. *J. Phys. Chem. B* **1999**, *103*, 608.
(32) Toan, N. M.; Morrison, G.; Hyeon, C.; Thirumalai, D. *J. Phys. Chem. B* **2008**, *112*, 6094.
(33) Wang, Z. S.; Makarov, D. E. *J. Chem. Phys.* **2002**, *117*, 4591.
(34) Wilemski, G.; Fixman, M. *J. Chem. Phys.* **1974**, *60*, 866.
(35) Perico, A.; Beggiato, M. *Macromolecules* **1990**, *23*, 797.
(36) Perico, A.; Cuniberti, C. *J. Polym. Sci.: Polym. Phys. Ed.* **1977**, *15*, 1435.
(37) Friedman, B.; O'Shaughnessy, B. *Phys. Rev. A* **1989**, *40*, 5950.
(38) Friedman, B.; O'Shaughnessy, B. *J. Phys. II* **1991**, *1*, 471.
(39) Friedman, B.; O'Shaughnessy, B. *Macromolecules* **1993**, *26*, 4888.
(40) Fernandez, J. L. G.; Rey, A.; Freire, J. J.; Pierola, I. F. d. *Macromolecules* **1990**, *23*, 2057.
(41) Ortiz-Repiso, M.; Freire, J. J.; Rey, A. *Macromolecules* **1998**, *31*, 8356.
(42) Ortiz-Repiso, M.; Rey, A. *Macromolecules* **1998**, *31*, 8363.
(43) Rey, A.; Freire, J. J. *Macromolecules* **1991**, *24*, 4673.
(44) Kim, J.-H.; Lee, W.; Sung, J.; Lee, S. *J. Phys. Chem. B* **2008**, *112*, 6250.

(45) Yeung, C.; Friedman, B. *J. Chem. Phys.* **2005**, *122*, 214909.
(46) Cheng, R. R.; Uzawa, T.; Plaxco, K. W.; Makarov, D. E. *J. Phys. Chem. B* **2009**, *113*, 14026.
(47) Szabo, A.; Schulten, K.; Schulten, Z. *J. Chem. Phys.* **1980**, *72*, 4350.
(48) Barzykin, A. V.; Seki, K.; Tachiya, M. *J. Chem. Phys.* **2002**, *117*, 1377.
(49) Portman, J. J.; Wolynes, P. G. *J. Phys. Chem. A* **1999**, *103*, 10602.
(50) Wang, J.; Wolynes, P. G. *Chem. Phys. Lett.* **1993**, *212*, 427.
(51) Wang, J.; Wolynes, P. G. *Chem. Phys.* **1994**, *180*, 141.
(52) DiMarzio, E. A. *J. Chem. Phys.* **1964**, *42*, 2101.
(53) De Gennes, P. G. *Scaling Concepts in Polymer Physics*; Cornell University Press: Ithaca, NY, 1979.
(54) Huang, L.; Makarov, D. E. *J. Chem. Phys.* **2008**, *128*, 114903.
(55) Doi, M.; Edwards, S. F. *The Theory of Polymer Dynamics*; Clarendon Press/Oxford University Press: Oxford [Oxfordshire]/New York, 1986.
(56) Kawakatsu, T. *Statistical Physics of Polymers*; Springer-Verlag: Berlin/Heidelberg, 2004.
(57) Des Cloizeaux, J.; Jannink, G. *Polymers in Solution: Their Modelling and Structure*; Clarendon Press: Oxford, 1990.
(58) Lapidus, L. J.; Eaton, W. A.; Hofrichter, J. *Phys. Rev. Lett.* **2001**, *87*, 258101.
(59) Tinland, B.; Pluen, A.; Sturm, J.; Weill, G. *Macromolecules* **1997**, *30*, 5763.

JP910669D